Microstructural Changes in β-Silicon Nitride Grains upon Crystallizing the Grain-Boundary Glass

William E. Lee[*,‡] and Gregory E. Hilmas[*,†]

Department of Materials Science and Engineering, The Ohio State University,
Columbus, Ohio 43210-1178

Crystallizing the grain-boundary glass of a liquid-phase-sintered Si_3N_4 ceramic for 2 h or less at 1500°C led to formation of δ-$Y_2Si_2O_7$. After 5 h at 1500°C, the δ-$Y_2Si_2O_7$ had transformed to β-$Y_2Si_2O_7$ with a concurrent dramatic increase in dislocation density within β-Si_3N_4 grains. Reasons for the increased dislocation density are discussed. Annealing for 20 h at 1500°C reduced dislocation densities to the levels found in as-sintered material. [Key words: silicon nitride, microstructure, grain boundaries, grains, glass.]

I. Introduction

THE predominantly covalent nature of the atomic bonds in Si_3N_4 hinders atom migration so that the solid-state sintering below the decomposition temperature (1878°C at atmospheric pressure in air[1]) is limited. Fabrication of structural components may therefore be facilitated by adding one or more oxides to the Si_3N_4 powder (e.g., Refs. 2 and 3), which combine with surface and (occasionally) added SiO_2 to form a low-melting-point silicate liquid. Liquid-phase sintering (LPS) occurs by a solution–reprecipitation mechanism as originally proposed by Drew and Lewis.[4] In this process the α-Si_3N_4 starting powder dissolves in the silicate liquid and is precipitated out as β-Si_3N_4, with the silicate liquid solidifying as a glass at the grain boundaries of the final product. Unfortunately, the low melting point of the silicate phase used to advantage during sintering is detrimental to the mechanical properties of the monolithic material at high temperatures, since the glass typically begins to soften at relatively low temperatures (about 1000°C).

One method of improving the high-temperature mechanical strength is to alter the glass composition to increase its softening point (e.g., Ref. 5). Another technique is to use a postsinter heat treatment to crystallize the glass to a more refractory phase. In a recent study[6] we employed the latter technique for Si_3N_4 fabricated with a Y_2O_3 sintering aid and crystallized $Y_2Si_2O_7$ at the grain boundaries. We present here observations of the effect of this crystallizing treatment on the microstructure of the β-Si_3N_4 grains.
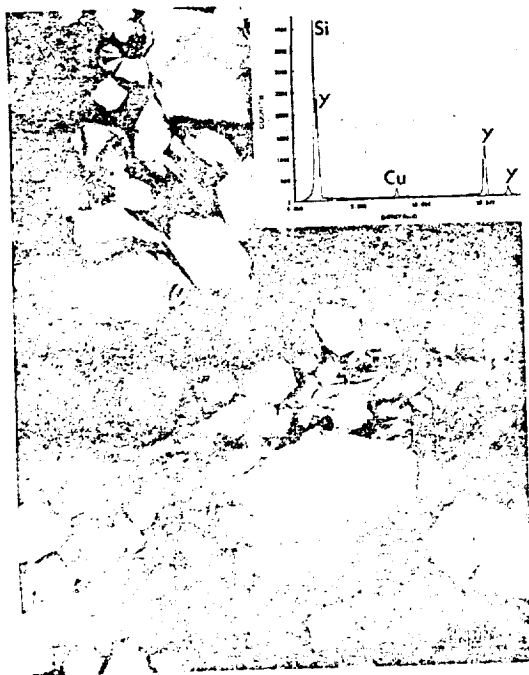

Fig. 1. Bright-field (BF) TEM image of the general microstructure of as-sintered Si_3N_4 with (inset) EDS spectrum from glassy phase.
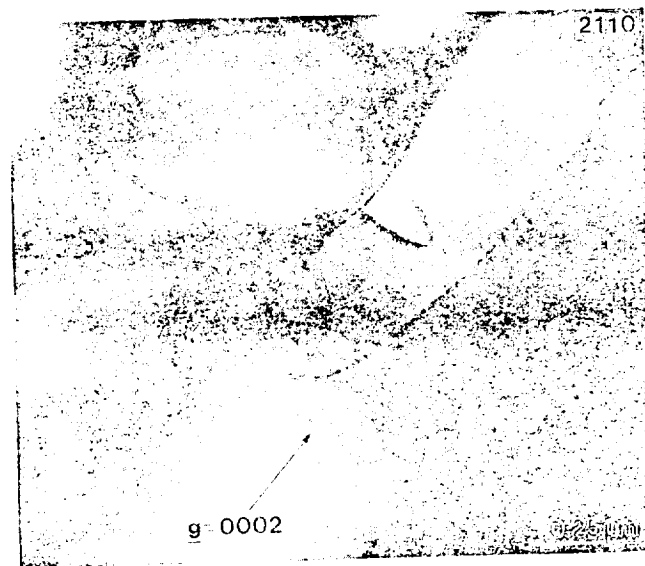

Fig. 2. BF TEM image of a group of $b = \langle 0001 \rangle$ dislocations in a β-Si_3N_4 grain of as-sintered material.

II. Experimental Procedure

The starting powders were Si_3N_4[‡] (83.7 wt% α, 15.7 wt% β, and 0.6 wt% Si), Y_2O_3,[§] and SiO_2.[*] The powders were mixed in the ratio 90:6.4:3.6 wt%, respectively, and milled as 100-g charges in 1-L Si_3N_4 mills using high-purity Si_3N_4 milling media and ethanol. After oven drying under vacuum, the powders were die-pressed into bars at 21 MPa followed by cold isostatic pressing at 414 MPa. These bars were then sintered at 2140°C for 4 h under 50 atm ($\approx$5 $\times$ 10⁶ Pa) of N_2. The crystallizing anneal was performed at 1500°C for times of 0.5, 2, 5, 10, and 20 h, again under 50 atm of N_2. The heating rate from room temperature to 1500°C was 42°C/min, while the cooling rate after switching off the furnace was 130°C/min.

Electron microscopy was performed using either of two TEM units[**] equipped with an EDS[††] system. TEM specimens were prepared using standard ceramographic techniques. First, 3-mm-diameter disks were ultrasonically cut from 1-mm-thick slices of the bars and ground and polished to 100 μm before dimpling to 20-μm-center thickness. Final polishing and dimpling was done with 3-μm diamond paste. Ion milling was performed using 6-kV Ar^+ ions. Dislocation Burgers vectors were determined using the $g \cdot b = 0$ invisibility criterion[7] where g is the operating reflection and b the Burgers vector of the dislocation. With this technique, dislocations must go out of contrast for two nonparallel reflections, and while the invisibility criterion is strictly valid only for pure screw dislocations, it is commonly applied to those containing an edge component where the contrast at the $g \cdot b = 0$ but $g \cdot b \times u \neq 0$ condition is minimal. Residual contrast can arise from the $g \cdot b \times u$ term and/or from elastic anisotropy and in some cases requires image-contrast calculations[8] to determine b. Image-matching calculations were not attempted here. Weak-beam dark-field (WBDF) imaging was necessary when examining dislocations in Si_3N_4. This technique[9] images only the dislocation core and enables high densities of dislocations to be studied. In conventional bright-field (BF) and dark-field (DF) images, the overlapping strain fields of the dislocations make analysis of them impossible. Diffraction patterns for Si_3N_4 were solved with the assistance of Ref. 10.

Dislocation densities for 100 adjacent grains were determined in each sample, using the method of counting intersections of dislocations with drawn circles as described in Ref. 7. Convergent beam electron diffraction[11] was used to measure the thickness of representative grains and an average value of 200 nm used in all density calculations. This will introduce some error in the dislocation density measurements. Further error is introduced because the technique of Hirsch *et al.*[7] leads to an underestimate of dislocation density, since at all orientations some dislocations will be out of contrast. This error was minimized by using $g = 0002$ at the [$1\bar{2}10$] zone axis whenever possible in images used for density determinations. At this orientation the majority of dislocations with $b = \langle 0001 \rangle$ or with c and a components in their b are in contrast but not those with $b = \frac{1}{3}[1\bar{2}10]$. The maximum total error associated with this procedure for dislocation densities is expected to be on the order of 25%.

III. Results

(1) As-Sintered Microstructure

A BF TEM image of the general microstructure is shown in Fig. 1. Hexagonal β-Si_3N_4 grains are contained in a glue of yttrium silicate glass. Other minor phases occasionally observed in the microstructure include α-Si_3N_4, β-SiC, and up to 5 vol% Si_2N_2O. An EDS spectrum from the glass is shown inset in Fig. 1. More detailed BF examination of the silicon nitride grains shows that some of them contain dislocations (Fig. 2) which we assume are simply "grown in" during the reprecipitation process. The distribution of dislocation densities in β-Si_3N_4 grains (Fig. 3(a)) reveals that about 60% of the grains do not contain dislocations and the maximum dislocation density observed in any grain is 31 $\times$ 10⁹/cm². Burgers vector (b) analysis on
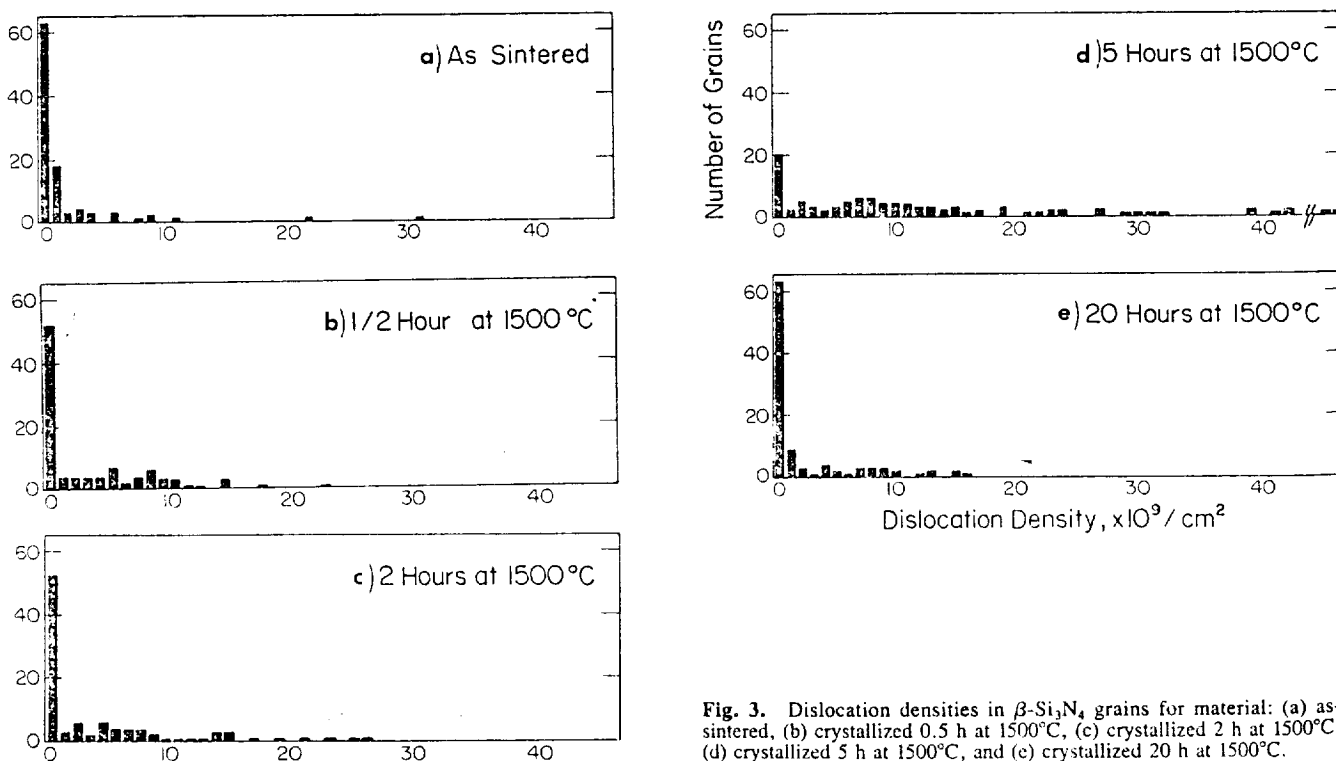
Fig. 3. Dislocation densities in β-Si_3N_4 grains for material: (a) as-sintered, (b) crystallized 0.5 h at 1500°C, (c) crystallized 2 h at 1500°C, (d) crystallized 5 h at 1500°C, and (e) crystallized 20 h at 1500°C.

Fig. 4. BF image of mottled morphology of δ-Y₂Si₂O₇ crystallized after 2 h at 1500°C. Inset is the [010] zone axis for δ-Y₂Si₂O₇; extra spots arise from other microcrystals included in the selected area aperture.

Fig. 5. BF image showing highly stressed microstructure of Si₃N₄ after 5 h at 1500°C. β-Y₂Si₂O₇ crystallizes at the grain boundaries. The [001] zone axis for β-Y₂Si₂O₇ is inset.

selected dislocations indicates that the vast majority of the dislocations have $b = \langle 0001 \rangle$. However, dislocations having other b's were occasionally observed; for example, some dislocations had $b = \frac{1}{3}\langle 1\bar{2}10 \rangle$.

(2) Microstructure After Heating 0.5 h at 1500°C

After crystallization for only 0.5 h at 1500°C, the microstructure was significantly altered. At the resolution utilized (about 1 nm) the glass had completely crystallized. Electron diffraction patterns matched δ-Y₂Si₂O₇ which had a "mottled" morphology in BF, described as "blocky" by Ref. 12, shown in Fig. 4. The dislocation density was slightly higher than in the as-sintered microstructure (Fig. 3(b)), with about 52% of the grains being dislocation-free.

(3) Microstructure After Heating 2 h at 1500°C

The microstructure after 2 h at 1500°C was essentially unchanged from that observed after the 0.5-h crystallizing heat treatment. The dislocation density is given in Fig. 3(c).

(4) Microstructure After Heating 5 h at 1500°C

After a crystallizing heat treatment of 5 h at 1500°C, a highly stressed microstructure is observed (Fig. 5), with large numbers of bend and strain contours visible in the silicon nitride grains. As discussed in Ref. 6, the glassy grain-boundary phase has recrystallized to β-Y₂Si₂O₇ after this anneal, with no δ-Y₂Si₂O₇ remaining. The inset diffraction pattern in Fig. 5 is the [001] zone for β-Y₂Si₂O₇. WBDF imaging reveals that the strain contours arise from complicated and dense dislocation networks and tangles within the β-Si₃N₄ grains (Fig. 6). The distribution of dislocation densities (Fig. 3(d)) shows that now only about 20% of grains are dislocation-free, while the maximum density is $86 \times 10^9/\text{cm}^2$. Again the predominant b is $\langle 0001 \rangle$, as indicated by the Burgers vector analysis of Fig. 7 (see the g · b, Table I), in which all dislocations are in contrast for g = 0002 and 0$\bar{1}$11 but invisible for 3$\bar{6}$30 and 1$\bar{3}$20. The heterogeneous nature of the dislocation distribution should be emphasized here in that a dislocation-free grain is often found next to a highly dislocated grain, with no gradual change apparent. Preparation of TEM specimens from material after this treatment was more difficult

than for material given any other treatment; samples invariably cracked on ion thinning.

(5) Microstructure After Heating 20 h at 1500°C

Long heat treatment times at 1500°C led to reduced dislocation densities (Fig. 3(e)), presumably due to the dislocations annealing out. However, the dislocations remaining had undergone extensive rearrangement during the longer heat treatment, giving
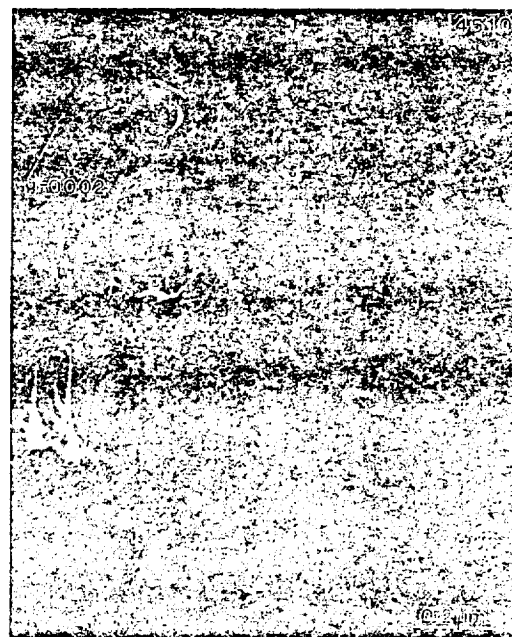

Fig. 6. WBDF image of dense dislocation tangles found after 5 h at 1500°C.
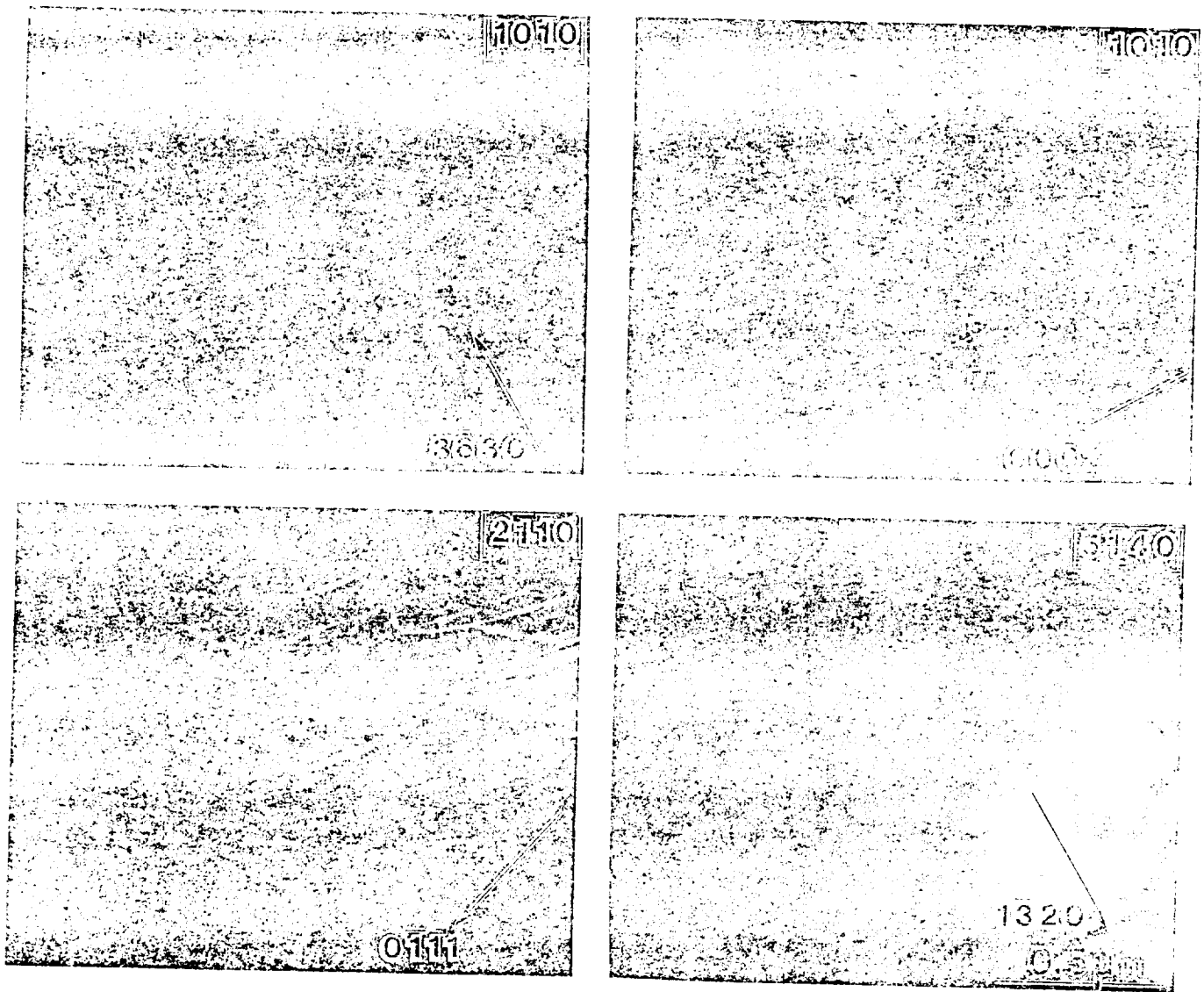
Fig. 7. Burgers vector analysis of dislocations after 5 h at 1500°C using $g = 3\bar{6}30$ and 0002 from the [10$\bar{1}$0] zone, $g = 0\bar{1}11$ from [2$\bar{1}\bar{1}$0], and $g = 1\bar{3}20$ from [5$\bar{1}40$]. All dislocations in this area have $b = \langle 0001 \rangle$.

rise to morphologies such as those of Fig. 8. The Burgers vector analysis illustrated in Fig. 8 suggests that a large number of the dislocations still have $b = \langle 0001 \rangle$, i.e., those in contrast for $g = 0002$ and $0\bar{1}1\bar{1}$ but out for $g = 3\bar{6}30$ and $02\bar{2}0$, e.g., A. However, dislocations having other b's are present. If we consider only the perfect dislocation listed for hexagonal structures in Table I, other possible b's are $\frac{1}{3}\langle 2\bar{1}\bar{1}3 \rangle$, e.g., B (in contrast for 0002, $0\bar{1}1\bar{1}$, and $3\bar{6}30$ but out for $02\bar{2}0$), and $\frac{1}{3}[\bar{2}110]$, e.g., C (in contrast for $g = 3\bar{6}30$ but out for $0\bar{1}1\bar{1}$, 0002, and $02\bar{2}0$).

(6) Sub-Grain Boundaries and Polygonized Networks

All samples contained occasional examples of dislocation networks and sub-grain boundaries, e.g., Fig. 9. Initial attempts at b analysis suggest that many of these boundaries are complicated and may require comparison to calculated images for complete interpretation. This is beyond the scope of the present study but will be pursued in the future.

IV. Discussion

Crystallization of the grain-boundary glass to increase the refractoriness of Si_3N_4 ceramics has been intensively studied since the initial work of Tsuge et al.,[13] also on the Y_2O_3–Si_3N_4 system. However, this is the first observation that crystallization of the

grain-boundary phase may have an effect on the Si_3N_4 grains. While some caution must be heeded with these data in that, because of the complexity of the experiments, only 100 grains were examined in each sample, the trends observed were reproducible. Several explanations can be proffered for the appearance of the dislocations, including a volume change on crystallizing the glass, a volume change upon transformation of one polymorphic form of the crystalline phase to another, or a difference between the thermal expansion coefficient of the phases present.

While the densities of the $Y_2Si_2O_7$ polymorphs are available (see Ref. 14 and Table II), the density of $Y_2Si_2O_7$ glass is not, and experiments to fabricate it and measure its density have been unsuccessful.[15] Crystallization of a glass, however, usually leads to a reduction in volume due to the closer packing of atoms in a crystalline structure, and it seems likely that a volume decrease will occur. Any volume change (increase or decrease) in the grain-boundary phase will impose a strain on the Si_3N_4 grains, deforming them and creating dislocations. The slight increase in dislocation density in the sample crystallized for 0.5 h compared to the as-sintered sample (Figs. 3(a) and (b)) may be attributed to this.

However, the biggest increase in dislocation density occurs between 2 and 5 h at 1500°C (Figs. 3(c) and (d)), during which time, as revealed by electron diffraction analysis, the grain-
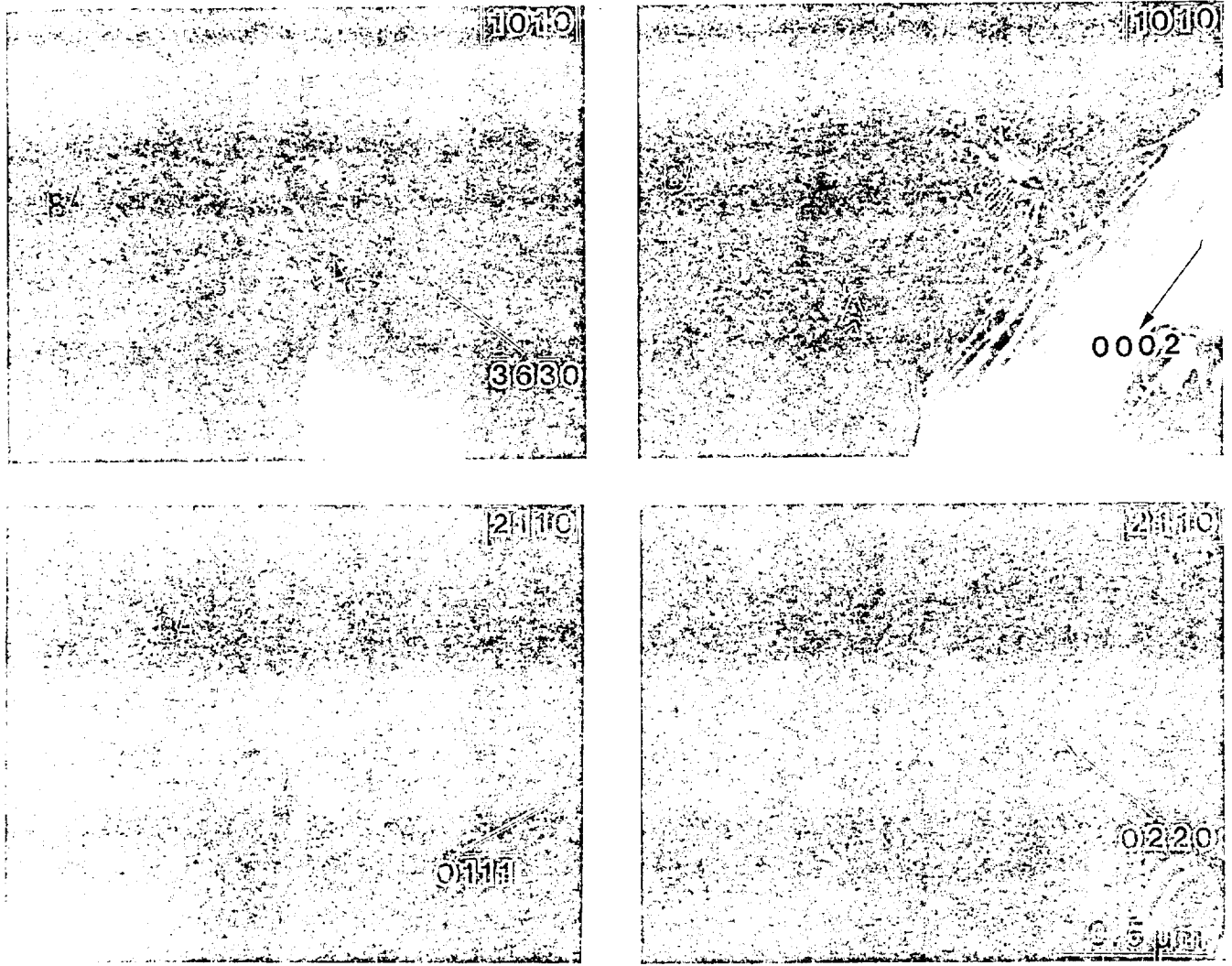
Fig. 8. Partial Burgers vector analysis of dislocations after 20 h at 1500°C using $g = \bar{3}6\bar{3}0$ and 0002 from the $[10\bar{1}0]$ zone and $g = 0\bar{1}1\bar{1}$ and $02\bar{2}0$ from $[\bar{2}110]$. Arrowed dislocations have $b = \langle 0001\rangle$ (A), $\frac{1}{3}[2\bar{1}\bar{1}3]$ (B), and $\frac{1}{3}[\bar{2}110]$ (C).

boundary phase transforms from δ- to β-Y₂Si₂O₇. This strongly suggests that a volume change associated with this transformation is responsible for the observed stress and dislocation formation after 5 h at 1500°C. The volume changes between the polymorphs in Y₂Si₂O₇ are given in Table III, calculated from data in Ref. 14. As can be seen, the largest volume change on any transformation is for $\alpha = \beta$. However, the nearly 2% volume change associated with the δ-to-β transition could well generate the stresses necessary to deform the Si₃N₄ grains at 1500°C. Any

shear associated with the δ-to-β transition, which is from orthorhombic to monoclinic symmetry (see Table II), could also contribute to dislocation formation. The dislocation microstructures formed in the crystallized material are typical of those induced in ceramics by high-temperature deformation.[16] The reduced dislocation density after 20 h at 1500°C is due to annealing out of the dislocations by the prolonged heat treatment (Fig. 3(e)).

According to Liddel and Thompson,[14] α-Y₂Si₂O₇, the low-temperature form, transforms to β at 1225°C, which should trans-

Table I. Values of $g \cdot b$ for Relevent Reflections in the Hexagonal Crystal Structure for Perfect Dislocations

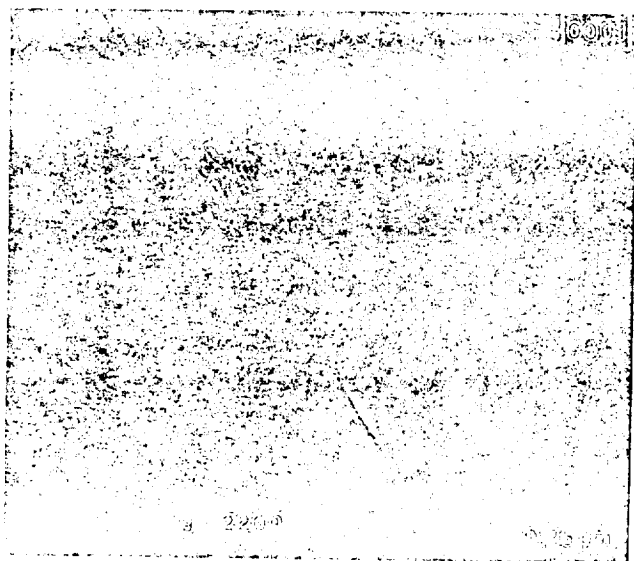| $b(\times 1/3)$	$20\bar{2}0$	$02\bar{2}0$	$2\bar{2}00$	0002	$63\bar{3}0$	$\bar{3}6\bar{3}0$	$33\bar{6}0$	$0\bar{1}1\bar{1}$	$0\bar{1}11$	$1\bar{3}20$
$\mp[11\bar{2}0]$	∓ 2	∓ 2	0	0	∓ 3	∓ 3	∓ 6	∓ 1	∓ 1	∓ 2
$\mp[\bar{1}2\bar{1}0]$	0	∓ 2	∓ 2	0	∓ 3	∓ 6	∓ 3	∓ 1	∓ 1	∓ 3
$\mp[\bar{2}110]$	∓ 2	0	∓ 2	0	∓ 6	∓ 3	∓ 3	0	0	∓ 1
$\mp[0003]$	0	0	0	∓ 2	0	0	0	∓ 1	∓ 1	0
$\mp[\bar{1}\bar{1}23]$	∓ 2	∓ 2	0	∓ 2	∓ 3	∓ 3	∓ 6	0	∓ 2	∓ 2
$\mp[\bar{1}2\bar{1}3]$	0	∓ 2	∓ 2	∓ 2	∓ 3	∓ 6	∓ 3	∓ 2	0	∓ 3
$\mp[\bar{2}1\bar{1}3]$	∓ 2	0	∓ 2	∓ 2	∓ 6	∓ 3	∓ 3	∓ 1	∓ 1	∓ 1
$\mp[\bar{1}\bar{1}23]$	∓ 2	∓ 2	0	∓ 2	∓ 3	∓ 3	∓ 6	∓ 2	0	∓ 2
$\mp[\bar{1}2\bar{1}3]$	0	∓ 2	∓ 2	∓ 2	∓ 3	∓ 6	∓ 3	0	∓ 2	∓ 3
$\mp[2\bar{1}\bar{1}3]$	∓ 2	0	∓ 2	∓ 2	∓ 6	∓ 3	∓ 3	∓ 1	∓ 1	∓ 1

Fig. 9. WBDF image of a sub-grain boundary and a polygonized network (arrowed) in a β-Si$_3$N$_4$ grain imaged using g = 2200 at the [0001] orientation. The edges of the hexagon are the projections of {10$\bar{1}$0} planes.

form to γ at 1445°C. Possible reasons for the observation that γ was never detected in the room-temperature microstructure after heat treatment at 1500°C are discussed at length by Lee et al.[17]

The thermal expansion coefficient of Y$_2$Si$_2$O$_7$ is not available, while that of β-Si$_3$N$_4$ is known to be low but highly anisotropic.[18] For the temperature range 0° to 1000°C, the thermal expansion coefficient is 3.23×10^{-6}/°C along the a axis and 3.72×10^{-6}/°C along the c axis. This anisotropy is expected to remain at temperatures up to the crystallization temperature used in this study (1500°C) and may cause a significant amount of stress on a local scale, especially if the thermal expansion coefficient of Y$_2$Si$_2$O$_7$ is also anisotropic. Thermal expansion mismatch, however, would be expected to lead to similar stress and consequent dislocation formation in all samples regardless of hold time at temperatures, since the stress arises only during the heating and cooling cycle. This cannot, therefore, be invoked to explain the much higher dislocation densities observed after a 5-h crystallization treatment as compared to material receiving other treatments.

Tighe[19] used TEM to examine the surface of Si$_3$N$_4$ bars which had been ground with 400-mesh SiC and found high dislocation densities and cracking to a depth of several micrometers. However, after polishing using unreported conditions the damage was substantially reduced. While the possibility exists that some of the dislocations observed in the present study arose from deformation during TEM specimen preparation, it seems unlikely that it could explain the trends observed as a function of heat treatment time, since all samples were prepared in the same manner. The preparation techniques used in the present study did not stop at 400-mesh SiC but continued to 600-mesh SiC followed by polishing with 15-, 9-, and 6-μm diamond paste. The final polish

and dimple then utilized 3-μm diamond paste. This procedure would not be expected to induce severe surface damage in Si$_3$N$_4$ at room temperature.

The observation that TEM specimens of the material with high dislocation density fractured on ion thinning is an indication that the room-temperature mechanical properties may be adversely affected by the stress present. However, further mechanical testing of material after the various heat treatments is needed to corroborate this, although the fact that the dislocations anneal out after longer heat treatment times suggests any deterioration may only be temporary. Previous detailed studies of dislocations in Si$_3$N$_4$ are sparse, although many authors have commented on the presence of dislocations in Si$_3$N$_4$ samples (e.g., Ref. 20). Evans and Sharp,[21,22] Butler,[23] and Kossowsky[24] analyzed the Burgers vectors of dislocations in hot-pressed and reaction-bonded materials. In both forms, most of the dislocations had a (0001)-type b, although other types of dislocation containing an $a + c$ axis component b were present, tentatively identified as having b approximately $\frac{1}{3}$(11$\bar{2}$3) by Evans and Sharp.[21] Consideration of the strain energy associated with various types of dislocation in Si$_3$N$_4$[21] indicated that (0001) was the most stable b, whereas an analysis of dislocation mobility using the Peierls model suggested they would also be the most mobile, with {10$\bar{1}$0} as the primary slip plane. The highly anisotropic slip on systems with a (0001) Burgers vector in Si$_3$N$_4$[21] could be used to explain the inhomogeneity of observations of grains containing dislocations. The observation of $\frac{1}{3}$(1$\bar{2}$10) and $\frac{1}{3}$(11$\bar{2}$3)-type b dislocations in the present study is interesting, and further study of dislocation reactions in this system seem warranted. Kossowsky et al.[25] suggested that dislocation motion was unlikely at temperatures <1700°C in Si$_3$N$_4$ and, therefore, their contribution to, for example, creep mechanisms would be small. Evans and Sharp,[21] however, identified dislocation motion associated with plastic deformation at 1400°C in reaction-bonded Si$_3$N$_4$. More recently Clarke[26] has detected increased dislocation densities in material that had undergone a creep test. We feel that more detailed analysis of the dislocations in Si$_3$N$_4$ is important since dislocations may well play an active role in high-temperature deformation mechanisms in both monolithic and composite Si$_3$N$_4$-containing materials.

V. Summary and Conclusions

Crystallizing the grain-boundary glass in a Si$_3$N$_4$ ceramic containing 6 wt% Y$_2$O$_3$ led to the formation of δ-Y$_2$Si$_2$O$_7$ after 0.5- or 2-h anneals at 1500°C. A slight increase in dislocation density in the β-Si$_3$N$_4$ grains was noted after crystallization. However, after a 5-h anneal at 1500°C the δ-Y$_2$Si$_2$O$_7$ had transformed to β-Y$_2$Si$_2$O$_7$, and associated with the transition was a dramatic increase in dislocation density in the β-Si$_3$N$_4$ grains. The most likely origin for the deformation of the silicon nitride grains is the volume change accompanying the δ-to-β-Y$_2$Si$_2$O$_7$ transition. Longer anneals at 1500°C for times up to 20 h reduced the dislocation density to the levels observed in as-sintered materials, suggesting that any affect on the mechanical properties of the silicon nitride may be removed.

Table II. Space Groups, Specific Volumes, and Densities for the Y$_2$Si$_2$O$_7$ Polymorphs

Polymorph	Space group	Specific vol (nm^3)	Density (g/cm^3)
Y	Monoclinic $P2_1/m$*	0.1407	4.083
α	Triclinic $P\bar{1}$	0.1336	4.300
β	Monoclinic $C2/m$	0.1425	4.032
γ	Monoclinic $P2_1/n$	0.1422	4.040
δ	Orthorhombic $Pna2_1$	0.1398	4.110

*Determined as $Aba2$ by Ref. 12.

Table III.   Volume Changes Associated with Transformations between Y₂Si₂O₇ Polymorphs on Heating

Polymorphs	Vol change (%)
$\alpha \rightarrow \beta$	+6.233
$\beta \rightarrow \gamma$	−0.198
$\gamma \rightarrow \delta$	−1.733
$\beta \rightarrow \delta$	−1.984

References

[1]S. C. Singhal, "Thermodynamic Analysis of the High-Temperature Stability of Si₃N₄ and SiC," *Ceramurgia Int.*, **2** [3] 123–30 (1976).

[2]G. G. Deeley, J. M. Herbert, and N. C. Moore, "Dense Silicon Nitride," *Powder Metall.*, **8**, 145–51 (1961).

[3]A. Tsuge and K. Nishida, "High Strength Hot-Pressed Si₃N₄ with Concurrent Y₂O₃ and Al₂O₃ Additions," *Am. Ceram. Soc. Bull.*, **57** [4] 424–26, 431 (1978).

[4]P. Drew and M. H. Lewis, "The Microstructures of Silicon Nitride Ceramics During Hot-Pressing Transformations," *J. Mater. Sci.*, **9**, 261–69 (1974).

[5]R. E. Loehman, "Preparation and Properties of Yttrium-Silicon-Aluminum Oxynitride Glasses," *J. Am. Ceram. Soc.*, **62** [9–10] 491–94 (1979).

[6]W. E. Lee, C. H. Drummond III, G. E. Hilmas, J. D. Kiser, and W. A. Sanders, "Microstructural Evolution on Crystallizing the Glassy Phase in a 6 wt% Y₂O₃ Si₃N₄ Ceramic," *Ceram. Eng. Sci. Proc.*, **9** [9–10] 1355–66 (1988).

[7]P. B. Hirsch, A. Howie, R. B. Nicholson, D. W. Pashley, and M. J. Whelan, Electron Microscopy of Thin Crystals. Kreiger, New York, 1977.

[8]A. K. Head, P. Humble, L. M. Clareborough, A. J. Morton, and C. T. Forwood, Computed Electron Micrographs and Defect Identification. North-Holland, Amsterdam, 1973.

[9]D. J. H. Cockayne, I. L. F. Ray, and M. J. Whelan, "Investigations of Dislocation Strain Fields Using Weak Beams," *Philos. Mag.*, **20** [168] 1265–70 (1969).

[10]J. V. Sharp, A. G. Evans, and B. Hudson, "Electron Diffraction Data for Silicon Nitride," Harwell Research Report AERE-R7319, 1972.

[11]S. A. Allen, "Foil Thickness Measurements from Convergent-Beam Diffraction Patterns," *Philos. Mag. A*, **43** [2] 325–35 (1981).

[12]T. R. Dinger, R. S. Rai, and G. Thomas, "Crystallization Behavior of a Glass in the Y₂O₃–SiO₂–AlN System," *J. Am. Ceram. Soc.*, **71** [4] 236–44 (1988).

[13]A. Tsuge, K. Nishida, and M. Komatsu, "Effect of Crystallizing the Grain-Boundary Glass Phase on the High-Temperature Strength of Hot-Pressed Si₃N₄ Containing Y₂O₃," *J. Am. Ceram. Soc.*, **58** [7–8] 323–26 (1975).

[14]K. Liddel and D. P. Thompson, "X-ray Diffraction Data for Yttrium Silicates," *Br. Ceram. Trans. J.*, **85**, 17–22 (1986).

[15]M. Long; private communication.

[16]T. E. Mitchell, "Application of Transmission Electron Microscopy to the Study of Deformation in Ceramic Oxides," *J. Am. Ceram. Soc.*, **62** [5–6] 254–67 (1979).

[17]W. E. Lee, C. H. Drummond III, G. E. Hilmas, and S. Kumar, "A Comparison of the Crystallization Behavior of Y₂O₃–SiO₂ Glass as Bulk Material and as an Intergranular Phase in Si₃N₄"; unpublished work.

[18]C. M. B. Henderson and D. Taylor, "Thermal Expansion of the Nitrides and Oxynitride of Silicon in Relation to Their Structures," *Br. Ceram. Trans. J.*, **74**, 49–53 (1975).

[19]N. J. Tighe, "Characterization of Flaws Produced by Mechanical Grinding of Si₃N₄"; pp. 144–45 in Proceedings of the 35th Annual Meeting of the Electron Microscopy Society of America (EMSA). San Francisco Press, San Francisco, CA, 1977.

[20]H. Makino, N. Kamiya, and S. Wada, "Strength Degradation of Si₃N₄ by Contact Stress," *J. Mater. Sci. Lett.*, **7**, 475–76 (1988).

[21]A. G. Evans and J. V. Sharp, "Transmission Electron Microscopy of Silicon Nitride"; pp. 1141–53 in Electron Microscopy and Structure of Materials. Edited by G. Thomas, R. M. Fulrath, and R. M. Fisher. California Press, Berkeley, CA, 1972.

[22]A. G. Evans and J. V. Sharp, "Microstructural Studies on Silicon Nitride," *J. Mater. Sci.*, **6**, 1292–302 (1971).

[23]E. Butler, "Observations of Dislocations in β-Silicon Nitride," *Philos. Mag.*, **24**, 829–34 (1971).

[24]R. Kossowsky, "The Microstructure of Hot-Pressed Silicon Nitride," *J. Mater. Sci.*, **8**, 1603–15 (1973).

[25]R. Kossowsky, D. G. Miller, and E. S. Diaz, "Tensile and Creep Strengths of Hot-Pressed Si₃N₄," *J. Mater. Sci.*, **10**, 983–97 (1975).

[26]D. R. Clarke; private communication.   □

journal

Microstructural Evolution in Near-Eutectic Yttrium Silicate Compositions Fabricated from a Bulk Melt and as an Intergranular Phase in Silicon Nitride

William E. Lee,*,* Charles H. Drummond III,* Gregory E. Hilmas,*,† and Suresh Kumar*,‡

Department of Materials Science and Engineering, The Ohio State University, Columbus, Ohio 43210

Near-eutectic composition Y_2O_3–SiO_2 melts were formed as bulk samples or as an intergranular phase in Si_3N_4. Upon cooling to room temperature the bulk material partially crystallized to δ-$Y_2Si_2O_7$ whereas the intergranular phase was glass. On heat-treating at 1500°C the bulk material transformed to γ-$Y_2Si_2O_7$ whereas the intergranular glass crystallized first to δ-$Y_2Si_2O_7$, and then to β-$Y_2Si_2O_7$. Possible reasons for the different behavior are discussed. [Key words: crystallization, glass, yttria, silica, silicon nitride.]

I. Introduction

TO FACILITATE liquid-phase sintering (LPS) a metal oxide, or a mixture of oxides, is added to α-Si_3N_4 powder. The ubiquitous silica film present on the nitride particles (occasionally with added silica powder) combines with the oxide to form a low melting temperature liquid phase which is the host for the solution–reprecipitation sintering mechanism[1] known to occur in this material. The liquid composition influences its viscosity and hence the kinetics of sintering.[2,3] Sintering is carried out at high temperatures (>1700°C) in nitrogen atmospheres to retard decomposition of silicon nitride. Upon cooling to room temperature the silicate liquid has usually solidified to a glass and the α-Si_3N_4 powder has converted to β-Si_3N_4 during the solution–reprecipitation process. Unfortunately, the low melting temperature of the silicate phase, used to advantage during sintering, is detrimental to the mechanical properties of the monolithic material at elevated use temperatures since the glass begins to soften. This softening can promote grain-boundary sliding, cavitation creep, and subcritical crack growth at relatively low temperatures (about 1000°C).

The compositions of intergranular silicate glasses formed with various oxide additions have been examined using a range of analytical techniques such as analytical electron microscopy,[1,4,6] electron probe microanalysis,[7] and Auger electron spectroscopy.[7,8] Several authors[8-10] have even attempted to examine the properties of bulk glass fabricated with the approximate composition of the intergranular glass. These studies indicate that the presence of nitrogen not only increases the viscosity of the melt but also increases the glass transition temperature, hardness, density, and fracture toughness of the bulk glass at room temperature. Consequently, ni-

trogen incorporation in the intergranular silicate phase is envisaged as a route to improved high-temperature properties in silicon nitride based ceramics. Crystallization of the intergranular glass by pre-[11] or postsinter[12-14] heat treatments can also lead to improved high-temperature behavior by formation of a more refractory phase at the grain boundaries. No studies, however, have been made of the crystallization behavior of intergranular glass and bulk glass of the same composition. Microstructural characterizations of the crystallization of large volumes of bulk glass are more straightforward since the very high resolution analytical techniques (such as convergent beam electron diffraction, structure imaging, and field emission energy dispersive spectroscopy) needed to study small intergranular phases may be avoided. If the microstructural evolution of intergranular and bulk material can be shown to be equivalent, then use of the latter for phase stability studies is envisaged. This communication reports an attempt to compare the crystallization of an yttrium silicate melt in bulk form and as an intergranular phase in LPS silicon nitride.

II. Experimental Procedure

Bulk melts were prepared from 50-g batches of Y_2O_3§ and SiO_2¶ powder which were wet ball-milled in silicon nitride mills for 4 h using high-purity Si_3N_4 milling media and ethanol. After drying and dry milling for 2 h the batch was pressed into pellets at 10.3 MPa and melted in W crucibles at 2100°C for 4 h under 50 atm (about 5 MPa) of nitrogen. The heating rate was 45°C/min and the cooling rate was 520°C/min for the first minute after switching off the furnace and 170°C/min averaged over the next 10 min. The melt composition was chosen to be at the eutectic in the Y_2O_3–SiO_2 phase diagram. NASA 6Y composition silicon nitride samples[15] were prepared from Si_3N_4,** Y_2O_3,§ and SiO_2†† powders mixed in the weight ratio 90:6.4:3.6, respectively, and 100-g batches were milled for 300 h in 1-L silicon nitride ball mills again using high-purity Si_3N_4 milling media and ethanol. This milling process is known to increase SiO_2 content by about 1 to 2 wt% because of the oxidation of silicon nitride.[15] After drying, the powders were die-pressed into 3 cm × 0.56 cm × 0.28 cm bars at 21 MPa, cold isostatically pressed at 414 MPa, and sintered at 2140°C for 4 h under 50 atm (about 5 MPa) of nitrogen. Heating and cooling rates were the same as for the bulk material. Crystallizing anneals at 1500°C were in air for the bulk material (heating rate 10°C/min, cooling rate 20°C/min) but 50 atm of N_2 for the silicon nitride (heating and cooling rates as for sintering).

The elemental content of the bulk material (Table I) was determined by X-ray fluorescence (XRF) for all elements except N, which was determined by inert gas fusion (IGF). The composition of the intergranular glass was calculated from

Table I. Chemical Composition of the Bulk and Intergranular Glass

	Composition (wt%)			
	Y_2O_3	SiO_2	WO_3/W	N
As-mixed powder (bulk glass)	59.4	40.6	0	0
As-melted bulk glass by XRF and IGF*	60.96	39.94	0.92/0.73	0.12
As-mixed powder (intergranular)†	64.0	36.0	0	0

*Values total 101.75%, indicating a small error associated with the analytical techniques. †Not including oxide impurity and oxidation of Si_3N_4 powder during milling.

the starting powders (Table I). Allowing for SiO_2 impurity and oxidation of Si_3N_4 during milling, the final composition is expected to be close to the eutectic. Intergranular glass composition was also determined using energy dispersive X-ray spectroscopy (EDS) assuming oxides and ignoring the presence of N, which cannot be detected with a Be-window EDS detector. Microstructural and crystallographic analysis was performed using a transmission electron microscope[‡‡] (TEM) equipped with a Be-window EDS detector[§§] and an X-ray powder diffractometer[¶¶] using $CuK\alpha$ radiation. Electron energy loss spectroscopy[***] (ELS) was carried out at NASA Lewis Research Center.

III. Results and Discussion

(1) Bulk and Intergranular Melts on Cooling

After bulk powders were melted (at 2100°C) and Si_3N_4 bars were sintered (at 2140°C), furnace-cooled samples were examined using XRD. The bulk powders partially crystallized to δ-$Y_2Si_2O_7$ (Fig. 1(a)), the highest-temperature polymorph according to Refs. 16 and 17 (Table II). Some remnant silica glass is expected since this eutectic composition is richer in silica than pure $Y_2Si_2O_7$. Dinger et al.[18] found crystals of δ- or β-$Y_2Si_2O_7$ in as-melted bulk material of similar composition near the Y_2O_3–SiO_2 binary in their study of Y_2O_3–SiO_2–AlN glasses. The as-melted bulk sample contained about 0.73 wt% W (presumably present as WO_3) and a small amount (0.12 wt%) of nitrogen (Table I), attributed to contamination by container and nitrogen atmosphere, respectively.

The 6Y composition Si_3N_4, however, only contained XRD peaks from β-Si_3N_4. Electron diffraction and EDS analysis in the TEM confirmed that the intergranular phase was amorphous with a Si/Y ratio similar to that obtained by XRF for

Fig. 1. XRD spectra for (a) as-melted bulk sample, (b) bulk melt after 5 h at 1500°C in air, (c) intergranular glass after 5 h at 1500°C in 50 atm of nitrogen.

the eutectic composition bulk material (Table I). ELS analysis for nitrogen in the intergranular glass was inconclusive since the nitrogen edge could not be clearly distinguished from the background. This suggests that nitrogen is not present in large (i.e., >10 atom%) quantities upon cooling the melt to room temperature. Nitrogen will, however, be present in the silicate liquid at high temperatures from solution of α-Si_3N_4 powder and it is not surprising that many (determined at about 2 vol% from TEM images) lath-shaped Si_2N_2O grains were also detected in the as-sintered Si_3N_4 (Fig. 2). Si_2N_2O crystals, distinguishable by characteristic stacking faults along (100) planes,[19] reprecipitate along with β-Si_3N_4 grains. No evidence of any other devitrification was observed in the intergranular phase.

Assuming that the nitrogen content of the bulk material is low in the melt (otherwise Si_2N_2O would also have formed on cooling or high nitrogen contents would be present) the major chemical differences between the two melts are nitrogen content (higher in the intergranular melt) and the W/WO_3 impurity in the bulk melt. Oxynitride silicate melts are more viscous than the corresponding oxide melts. This is thought to be due to the incorporation of nitrogen capable of bridging three network tetrahedral groups replacing oxygen which is only capable of bridging two.[20] The higher viscosity of the intergranular melt may kinetically hinder crystallization of $Y_2Si_2O_7$ whereas the greater fluidity and presence of W/WO_3 in the bulk melt sample may tend to increase crystallization rates upon cooling. Neither the Si_3N_4 crystals nor any impurities scavenged by the silicate liquid[2] below the detection limit of EDS appear to facilitate crystallization of the intergranular glass on cooling.

The nitrogen contents are low in both bulk material (Table I) and intergranular glass (indicated by ELS analysis). Consequently, in the following discussion we will consider only the binary system Y_2O_3–SiO_2. In contrast to the yttrium SiAlONs, very little work has been published on the Y-Si-O-N system because of the difficulty of forming glasses. Drew et al.[9] obtained bloating and high weight loss due to nitrogen evolution when attempting to form glasses in this system, suggesting nitrogen incorporation in the glass, as opposed to the melt, is difficult.

(2) Heat Treatment at 1500°C

After 5 h at 1500°C δ-$Y_2Si_2O_7$ in the partially crystallized bulk sample had transformed to γ-$Y_2Si_2O_7$ (Fig. 1(b)) consistent with the polymorphism of $Y_2Si_2O_7$ given in Table II.

The 6Y-Si_3N_4 behaved very differently. After 2 h at 1500°C it had completely crystallized to δ-$Y_2Si_2O_7$ (Fig. 3), which is expected since crystallization of glasses often begins with metastable formation of the highest-temperature polymorph even at temperatures below its equilibrium field of stability.[21] Additional Si_2N_2O was also detected in the 6Y-Si_3N_4 after crystallization but with a different morphology than in as-sintered material (Fig. 4). In this case the Si_2N_2O is not present as lath-shaped grains but crystallized around Si_3N_4 grains although still with the characteristic (100) stacking faults and streaks in electron diffraction patterns. This crystallization and the observed morphology may result from formation of $Y_2Si_2O_7$, leaving a nitrogen-containing silica-rich glass which itself crystallized as Si_2N_2O. This result indicates that some nitrogen remained in the intergranular glass after cooling from the sintering temperature and was only incorporated
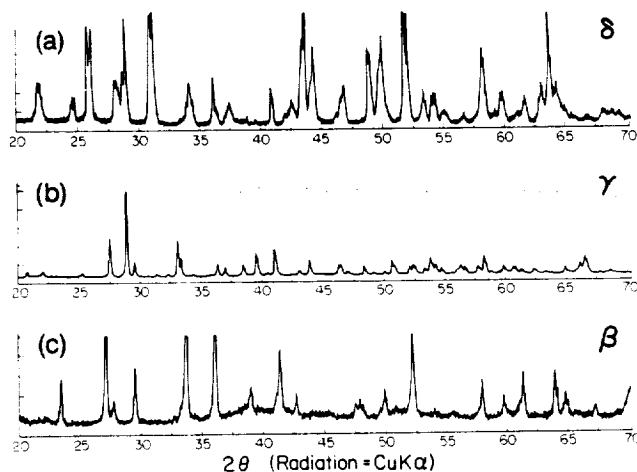
Table II. Physical and Crystallographic Data for the Polymorphs of $Y_2Si_2O_7$*

	Field of stability (°C)	Crystal system	Space group	a (nm)	b (nm)	c (nm)	α	β	γ	JCPDS file	Density (g·cm⁻³)
α	RT to 1225	Triclinic	$P\bar{1}$	0.659	0.664	1.225	94.0	89.2	93.1	21-1457	4.300
β	1225–1445	Monoclinic	$C2/m$	0.688	0.897	0.472	90	101.7	90	22-1103	4.032
γ	1445–1535	Monoclinic	$P2_1/n$	0.558	1.086	0.47	90	96.0	90	20-1436	4.040
δ	1535–1775	Orthorhombic	$Pna2_1$†	1.366	0.502	0.815	90	90	90	22-1460	4.110
Y	Impurity stabilized	Monoclinic	$P2_1/m$‡	0.75	0.806	0.502	90	112	90	32-1448	4.083

*Adapted from Refs. 16 and 17. †Reference 18 lists two δ polymorphs, δ_1 and δ_2, with δ_2 having space group $Pna2_1$. ‡Determined as $Aba2$ by Ref. 18 using convergent beam electron diffraction.

into Si_2N_2O crystallized with this morphology during heat treatment at 1500°C.

After 5 h at 1500°C the δ-$Y_2Si_2O_7$ had transformed to β-$Y_2Si_2O_7$ (Figs. 1(c) and 5), which remained even after 20 h at 1500°C. The 1.931% positive volume change associated with this transformation is thought to be responsible for the generation of large numbers of dislocations in the Si_3N_4 grains.[22] Transformation to β is unexpected since, according to the data in Table II, 1500°C is outside the field of stability of the β polymorph; instead δ would be expected to transform to γ at this temperature. As well as the differing initial phase assemblages, empirical differences between the crystallizing heat treatments for bulk and intergranular material include atmosphere (air and 50 atm of nitrogen, respectively) and quench rate (20° and 170°C/min, respectively). To test that these variables were not significant, bars of 6Y-Si_3N_4 were crystallized at 1500°C in the same furnace as the bulk glass, i.e., in air and with 20°C/min cooling rate. The $Y_2Si_2O_7$ polymorphs formed were the same as with the nitrogen atmosphere and the rapid quench rate.

While it may not be possible to state explicitly the reasons for the difference in behavior of the bulk and intergranular glass during postmelt heat treatments, several significant factors can be considered, such as impurity content, atmosphere, quench rate, crystal nucleation, the characteristics of the polymorphic transitions, and the presence or absence of quench crystals of δ-$Y_2Si_2O_7$. Admittedly much of what follows is conjecture since the information required to fully interpret the results is not available. For example, the effect of impurity ions on the polymorphism of $Y_2Si_2O_7$ has not been clarified and interfacial free energies are not available. However, the

following factors are expected to influence the crystallization behavior.

Intergranular glass in Si_3N_4 is known to scavenge impurity cations from the starting powders.[2] These impurities outdiffuse along the grain boundaries during elevated-temperature treatments. Falk[23] detected β-$Y_2Si_2O_7$ in grain boundaries at the near surface regions of Si_3N_4 bars but α in grain boundaries at depths near the bar center after 7 h at 1400°C in air. She attributes this result to stabilization of β by impurity cations outdiffusing during the heat treatment but also suggests that the annealing atmosphere may play a role in determining the particular polymorph which forms during crystallization. However, unpublished work by Kumar and Drummond found that the quench rate of melts was a more significant variable than nitrogen pressure. Melts in 1- or 50-atm nitrogen overpressures and quenched at different rates (110° and 170°C/min, respectively) contained similar amounts of nitrogen (about 0.1 wt%) but crystallized to the γ and δ polymorphs of $Y_2Si_2O_7$, respectively. As discussed above, the atmosphere and quench rate have less effect once crystals have formed. Incorporation of impurity cations is known to stabilize the Y form of $Y_2Si_2O_7$, which forms on oxidation of Y_2O_3-SiO_2 glasses[24] and β may be similarly stabilized. The observation that δ forms before β suggests that it too may be impurity stabilized.

Dinger et al.[18] found that Y-$S_2Si_2O_7$ nucleated on Fe-Si impurity particles in bulk glass and then transformed to δ-$Y_2Si_2O_7$ although they found two closely related but different polymorphs by HREM designated δ_1 and δ_2. Their results are also inconsistent with the stability fields of Ref. 17. This may

Fig. 2. Lath-shaped Si_2N_2O crystals in as-sintered 6Y-Si_3N_4.

Fig. 3. Dark-field TEM image of δ-$Y_2Si_2O_7$ crystals as intergranular phase in 6Y-Si_3N_4 after 2 h at 1500°C.

Fig. 4. Si_2N_2O crystallized around Si_3N_4 grains in $6Y$-Si_3N_4 after 5 h at 1500°C.

be due to the formation of metastable phases. The nucleation of crystals on impurities such as Fe-Si or W/WO_3 depends upon many factors, such as contact angle between nucleus and impurity substrate; impurity surface area, shape, and dispersion in the glass; lattice mismatch and interfacial free energy between the impurity and the nucleating crystal.[25] However, we observed no such microcrystals which might act as nucleants in the bulk melt glass of this study. In the intergranular glass the polymorph with the lowest interfacial free energy difference with respect to β-Si_3N_4 will crystallize as a transient or metastable phase if $Y_2Si_2O_7$ nucleates on Si_3N_4 grains. Support for the suggestion that β-Si_3N_4 favors the nucleation of β-$Y_2Si_2O_7$ was obtained by melting the eutectic glass composition at 2100°C for 4 h in 50 atm of nitrogen with a

6Y-Si_3N_4 bar and quenching. The resulting melt contained dissolved silicon nitride and only β-$Y_2Si_2O_7$.

The volume change on cooling associated with the δ-to-β transformation is 1.931% whereas it is 1.733% for the δ-to-γ transition so that it is unlikely that the volumetric constraint imposed by the Si_3N_4 grains would restrict one transformation in favor of the other. It is also unlikely that β is forming as a metastable phase en route to forming γ after sufficient time at temperature since β is a lower temperature polymorph and therefore less stable than γ at this temperature (Table II).

Some information on polymorphic transitions in other grain-boundary phases may also be gained from this study. The first polymorph to form upon crystallization, δ, has a characteristic mottled morphology and a small grain size, about 1 μm (Fig. 3), suggesting many nucleation sites are available (similar to cordierite crystallized in SiAlON grain boundaries[12]). However, after continued annealing at 1500°C the δ transforms to β with concurrent grain growth so that single grains of β-$Y_2Si_2O_7$ (about 10-μm diameter) extend over large volumes around many Si_3N_4 grains (Fig. 5). The greater grain size of β compared to δ suggests few β nuclei and/or rapid growth rates of the β nuclei present. If, as seems likely, the β grains nucleate on the δ grain boundaries, then rapid grain growth must be occurring. The large grains of garnet in SiAlON grain boundaries[12] may have formed in a similar manner.

IV. Summary and Conclusions

Attempts to form glass of identical composition from bulk melts and as an intergranular phase in Si_3N_4 were unsuccessful. While the intergranular material was amorphous, the bulk material contained crystals of δ-$Y_2Si_2O_7$ and a silicate glass at room temperature. On heat-treating at 1500°C the bulk material transformed to γ-$Y_2Si_2O_7$, whereas the intergranular glass crystallized first to δ-$Y_2Si_2O_7$ and then to β-$Y_2Si_2O_7$. Variables discussed which may explain the different behavior include impurity ions, impurity phases, and crystallographic factors. Quench rate and nitrogen content in the crystallization atmosphere were less significant variables.

Si_2N_2O forms in Si_3N_4 with two morphologies: as lath-shaped grains arising from nitrogen solution in as-sintered material (Fig. 2) and also crystallized around Si_3N_4 grains (Fig. 4) after a postsinter heat treatment. The latter morphology may arise since crystallization of $Y_2Si_2O_7$ leaves a N-containing silica-rich glass which itself crystallizes as Si_2N_2O.

Fig. 5. Dark-field TEM image of β-$Y_2Si_2O_7$ crystals as intergranular phase in 6Y-Si_3N_4 after 5 h at 1500°C.

References

[1]P. Drew and M. H. Lewis, "The Microstructures of Silicon Nitride Ceramics During Hot-Pressing Transformations," *J. Mater. Sci.*, **9**, 261–69 (1974).
[2]M. H. Lewis and R. J. Lumby, "Nitrogen Ceramics: Liquid Phase Sintering," *Powder Metall.*, **26** [2] 73–81 (1983).
[3]S. Hampshire and K. H. Jack, "The Kinetics of Densification and Phase Transformation of Nitrogen Ceramics," *Proc. Br. Ceram. Soc.*, **31** [6] 37–49 (1981).
[4]R. Kossowsky, "The Microstructure of Hot-Pressed Silicon Nitride," *J. Mater. Sci.*, **8**, 1603–15 (1973).
[5]D. R. Clarke, N. J. Zaluzec, and R. W. Carpenter, "The Intergranular Phase in Hot-Pressed Silicon Nitride: I, Elemental Composition," *J. Am. Ceram. Soc.*, **64** [10] 601–607 (1981).
[6]C. C. Ahn and G. Thomas, "Microstructure and Grain-Boundary Composition of Hot-Pressed Silicon Nitride with Yttria and Alumina," *J. Am. Ceram. Soc.*, **66** [1] 14–17 (1983).
[7]R. Kossowsky and S. C. Singhal; p. 275 in *Grain Boundaries in Engineering Materials*. Edited by J. L. Walter, J. H. Westbrook, and D. A. Woodford. Gaitors, Baton Rouge, LA, 1975.
[8]B. D. Powell and P. Drew, "The Identification of a Grain Boundary Phase in Hot-Pressed Silicon Nitride by Auger Electron Spectroscopy," *J. Mater. Sci.*, **9**, 1867–70 (1974).
[9]R. A. L. Drew, S. Hampshire, and K. H. Jack, "Nitrogen Glasses," *Br. Ceram. Soc. Proc.*, **31**, 119–32 (1981).
[10]R. E. Loehman, "Preparation and Properties of Yttrium-Silicon-Aluminum Oxynitride Glasses," *J. Am. Ceram. Soc.*, **62** [9–10] 491–94 (1979).

[11]A. Tsuge, K. Nishida, and M. Komatsu, "Effect of Crystallizing the Grain-Boundary Glass Phase on the High-Temperature Strength of Hot-Pressed Si_3N_4 Containing Y_2O_3," *J. Am. Ceram. Soc.*, **58** [7–8] 323–26 (1975).

[12]D. A. Bonnell, T.-Y. Tien, and M. Rühle, "Controlled Crystallization of the Amorphous Phase in Silicon Nitride Ceramics," *J. Am. Ceram. Soc.*, **70** [7] 460–65 (1987).

[13]L. K. L. Falk and G. L. Dunlop, "Crystallization of the Glassy Phase in an Si_3N_4 Material by Post-sintering Heat Treatments," *J. Mater. Sci.*, **22**, 4369–76 (1987).

[14]W. E. Lee, C. H. Drummond III, G. E. Hilmas, J. D. Kiser, and W. A. Sanders, "Microstructural Evolution on Crystallizing the Glassy Phase in a 6 wt% Y_2O_3–Si_3N_4 Ceramic," *Ceram. Eng. Sci. Proc.*, **9** [9–10] 1355–66 (1988).

[15]W. A. Sanders and G. Y. Baaklini, "Correlation of Processing and Sintering Variables with the Strength and Radiography of Silicon Nitride," *Ceram. Eng. Sci. Proc.*, **7** [7–8] 839–59 (1986).

[16]K. Liddell and D. P. Thompson, "X-ray Diffraction Data for Yttrium Silicates," *Trans. J. Br. Ceram. Soc.*, **85**, 17–22 (1986).

[17]J. Ito and H. Johnson, "Synthesis and Study of Yttrialite," *Am. Mineral.*, **53**, 1940–52 (1968).

[18]T. R. Dinger, R. S. Rai, and G. Thomas, "Crystallization Behavior of a Glass in the Y_2O_3–SiO_2–AlN System," *J. Am. Ceram. Soc.*, **71** [4] 236–44 (1988).

[19]M. H. Lewis, C. J. Reed, and N. D. Butler, "Pressureless-Sintered Ceramics Based on the Compound Si_2N_2O," *Mater. Sci. Eng.*, **71**, 87–94 (1985).

[20]R. E. Loehman, "Oxynitride Glasses," *Mater. Res. Bull.*, **12** [5] 26–30 (1987).

[21]G. O. Jones; p. 32 in *Glass*. Methuen, London, 1956.

[22]W. E. Lee and G. E. Hilmas, "Microstructural Changes in β-Silicon Nitride Grains upon Crystallizing the Grain-Boundary Glass," *J. Am. Ceram. Soc.*, **72** [10] 1931–37 (1989).

[23]L. K. L. Falk and G. L. Dunlop, "Crystallization of the Glassy Phase in an Si_3N_4 Material by Post-sintering Heat Treatments," *J. Mater. Sci.*, **22**, 4369–76 (1987).

[24]J. T. Smith, "Temperature and Compositional Stability of a $Y_6Si_6O_{21}$ Phase in Oxidized Si_3N_4," *J. Am. Ceram. Soc.*, **60** [9–10] 465–66 (1977).

[25]P. F. James, "Volume Nucleation in Silicate Glasses;" pp. 59–105 in *Glasses and Glass-Ceramics*. Edited by M. H. Lewis. Chapman and Hall, London, 1989. □